AD-A138 324 SPECTROSCOPIC INVESTIGATIONS OF MATERIALS FOR TUNABLE 1/1
INFRARED LASERS(U) OKLAHOMA STATE UNIV STILLWATER DEPT
OF PHYSICS R C POWELL 28 FEB 84 N00014-82-K-0109
UNCLASSIFIED F/G 20/5 NL

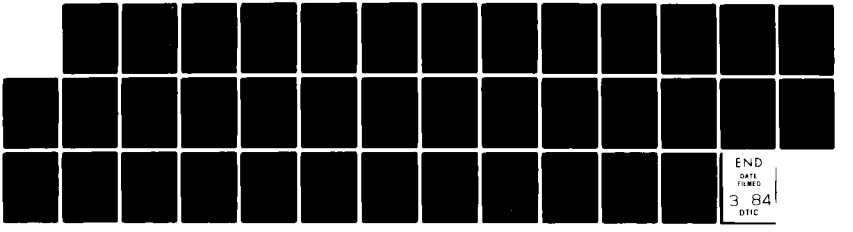

END
DATE FILMED
3 84
DTIC

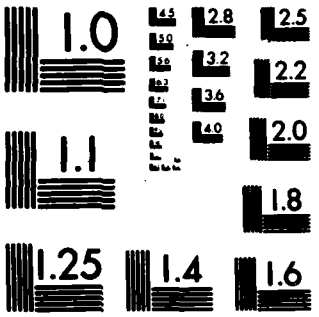

SECURITY CLASSIFICATION OF THIS PAGE (When Data Entered)

REPORT DOCUMENTATION PAGE

READ INSTRUCTIONS BEFORE COMPLETING FORM

1. REPORT NUMBER: 2	2. GOVT ACCESSION NO.
3. RECIPIENT'S CATALOG NUMBER	
4. TITLE (and Subtitle): Spectroscopic Investigations of Materials for Tunable Infrared Lasers	5. TYPE OF REPORT & PERIOD COVERED: Annual Progress Report No. 2, 1 March 1983-28 February 1984
	6. PERFORMING ORG. REPORT NUMBER
7. AUTHOR(s): Richard C. Powell	8. CONTRACT OR GRANT NUMBER(s): SFRC No.: N00014-82-K-0109
9. PERFORMING ORGANIZATION NAME AND ADDRESS: Department of Physics, Oklahoma State University, Stillwater, OK 74078	10. PROGRAM ELEMENT, PROJECT, TASK AREA & WORK UNIT NUMBERS: Project No.: NR 379-053/ 12-31-81
11. CONTROLLING OFFICE NAME AND ADDRESS: Office of Naval Research, Physics Division (Code 412), Dept. of the Navy, Arlington, Virginia 22217	12. REPORT DATE: 28 February 1984
	13. NUMBER OF PAGES: 36
14. MONITORING AGENCY NAME & ADDRESS(if different from Controlling Office): Office of Naval Research, Rm. 582, Federal Building, 300 E. 8th St., Austin, Texas 78701	15. SECURITY CLASS. (of this report): unclassified
	15a. DECLASSIFICATION/DOWNGRADING SCHEDULE

16. DISTRIBUTION STATEMENT (of this Report)

Approved for public release; distribution unlimited.

17. DISTRIBUTION STATEMENT (of the abstract entered in Block 20, if different from Report)

DTIC ELECTE FEB 2 8 1984 A

18. SUPPLEMENTARY NOTES

19. KEY WORDS (Continue on reverse side if necessary and identify by block number)

Lasers, Materials, Spectroscopy

20. ABSTRACT (Continue on reverse side if necessary and identify by block number)

This report describes research on the crystal growth and spectroscopic properties of 4d and 5d transition metal ions in halide and oxide host materials. Specific information is given on the fluorescence spectra and lifetimes of divalent Rh, Ru, Pt, and Ir ions in KBr and KCl crystals using time-resolved laser pumping. Differences is spectral properties of charge transfer and d level emission are reported as a function of temperature, annealing and radiation treatments. The spectral properties appear to be suitable for laser materials if higher concentrations of doping can be achieved.

DD FORM 1 JAN 73 1473 EDITION OF 1 NOV 65 IS OBSOLETE

S/N 0102-LF-014-6601

SECURITY CLASSIFICATION OF THIS PAGE (When Data Entered)

SPECTROSCOPIC INVESTIGATIONS OF MATERIALS

FOR TUNABLE INFRARED LASERS

ANNUAL PROGRESS REPORT No. 2
1 March 1983 - 28 February 1984

Principal Investigator:
Richard C. Powell
Department of Physics
Oklahoma State University

SFRC No. N00014-82-K-0109
Project No.: NR 379-053/12-31-81 410

During this time period, significant progress was made in developing the techniques of synthesizing alkali halide crystals containing 4d and 5d transition metal ions. Good optical quality single crystals of KCl, KBr, and $KMgF_3$ were grown with doping concentrations of the order of 200 ppm of divalent Ru, Rh, Ir, and Pt. Electron microprobe analysis and electron paramagnetic resonance measurements were performed to determine the approximate concentration, distribution and valence state of the dopant ions and the presence of any other optically active impurities. This was an important breakthrough for our research program considering the previous problems encountrered with the crystal growth of these materials and the failure of commercial crystal growth companies to produce samples of this type.

Detailed spectroscopic studies were performed on four samples: KBr:Pt, KBr:Rh, KCl:Ru, and KCl:Ir at temperatures between about 10 K and room temperature. Figures summarizing these results are attached to this report. For each sample there is a strong absorption transition in the near uv spectral region associated with charge transfer transitions which can be easily pumped with a N_2 laser. This results in two types of emission: a relatively narrow, very fast (~50 ns) band around 390 nm which is associated with charge transfer transitions; and a very broad, relatively slow (tens of microseconds) band peaking in the vicinity of 600 nm which is associated with d-d transitions. Both of these bands exhibit a significant amount of structure indicating the presence of several overlapping transitions due to crystal field splitting of the levels involved. The d-d emission appears to be associated with the lowest spin-allowed transitions

of the ions. No long-lived, near infrared emission due to spin forbidden d-d transitions could be detected.

As seen in the attached figures, the relative intensity of the d-d emission compared to the ct emission changes significantly as a function of temperature, annealing treatment, and radiation treatment. We also have observed a significant change in these relative intensities from host to host. Quantitative figures showing the temperature dependences of the lifetimes and relative intensities are attached. We are now in the process of interpreting these data in terms of rates of intersystem crossing from the ct system of energy levels to the d levels and in terms of radiationless relaxation among the d levels.

Some important preliminary conclusions can be drawn from these spectroscopic data:

(1) 4d and 5d transition metal ions can be incorporated into crystalline hosts and provide strong pump bands and broad emission bands ideal for tunable solid state laser materials.

(2) The peak emission cross section is estimated from spectral parameters to be of the order of 10^{-21} cm^2 which is similar to that of 3d transition metal ion vibronic lasers.

(3) The relatively fast decay time is better suited for laser pumping than for flash lamp pumping.

(4) The two key factors to making these materials work as lasers are: obtaining samples with increased doping ion

concentrations and maximizing the fraction of the emission that occurs in the d bands compared to the charge transfer bands.

During the coming year we plan to focus our work on two major areas. The first is to address the two problems mentioned in conclusion (4) above and to attempt to achieve single pass gain in KBr:Pt. If this is successful, further experiments on properties directly affecting laser performance such as excited state absorption and heat dissipation will be performed in an attempt to develop a N_2 laser pumped tunable solid state laser in the visible spectral region. The second area will be to try to obtain samples with strong intersystem crossing from the spin-allowed d levels to the low lying spin-forbidden d levels. There is some indication that this will occur in the oxide hosts. To try to accomplish this we are starting in-house oxide crystal growth of samples doped with these ions, working with Philips Research Laboratories to have some samples grown there, and working with scientists at Lawrence Livermore National Laboratory to have some ion-implanted samples prepared. The information we now have on the spectroscopy of these ions in alkali halide crystals indicates that in the right oxide host long-lived (millisecond times), broad band emission in the near infrared spectral region can be obtrained as initially predicted.

During this time period the principal investigator participated in the DARPA Workshop on Tunable Solid State Laser Materials and organized and chaired the invited symposium session on Tunable Solid State Laser Materials at the annual March Meeting of the American Physical Society. A formal presentation

of the word described here was made at the LASERS '83 meeting in San Fransisco (abstract attached) and a manuscript submitted for publication in the Journal of Chemical Physics (copy attached).

IV. OTHER INFORMATION

a. No technical papers or reports were published during this reporting period.

b. Student research assistants Xu Gang, G. Quarles, G. Gilliland, and L. Xi contributed to this research as did research associates J. Tyminski and G.E. Venikouas. C.A. Hunt and Prof. J.J. Martin assisted with the crystal growth.

c. No students earned degrees on this contract.

d. During this reporting period, the principal investigator also worked on three other projects:

"Use of Laser Spectroscopy Techniques for Investigating Radiationless Processes of Ions in Crystals"; National Science Foundation; $31,500 from 15 March 1983 to March 14, 1984.

"Spectroscopic Investigation of Materials for Frequency Agile Laser Systems"; Army Research Office; $71,586 from 15 January 1983 to 14 January 1984.

"Spectroscopic Properties of Optically Active Glasses"; Rome Air Development Center; $80,025 from 4 April 1983 to 3 April 1984; (with W.A. Sibley).

Talk presented at LASERS '83

SPECTROSCOPIC ANALYSIS OF 4d and 5d TRANSITION METAL IONS FOR TUNABLE SOLID STATE LASER MATERIALS*

R. C. Powell, J. J. Martin, R. H. Schweitzer, G. D. Gilliland

G. E. Venikouas and C. A. Hunt

Physics Department, Oklahoma State University, Stillwater, OK 74078

The optical spectra of ions such as divalent Rh, Ru, Pt, and Ir in alkali halide and oxide host crystals were investigated and the results interpreted in terms of the possible application of these materials as tunable solid state lasers.

*Work supported by contracts from the Office of Naval Research and the Army Research Office.

Submitted to J. Chem. Phys.

SPECTROSCOPY OF 4d AND 5d TRANSITION METAL IONS IN ALKALI HALIDE CRYSTALS

Richard C. Powell, Robert H. Schweitzer, Joel J. Martin, George E. Venikouas and Charles A. Hunt

Physics Department, Oklahoma State University, Stillwater, OK 74078

The fluorescence spectra and lifetimes of divalent Rh, Ru, Pt, and Ir ions in alkali halide crystals are measured using pulsed nitrogen laser excitation. Emission from both the charge transfer states and the excited d levels is observed. Changes in the relative intensities and lifetimes are monitored as a function of temperature, annealing, and radiation treatment. The results are interpreted in terms of the possible application of these materials for tunable solid state lasers.

I. INTRODUCTION

There is currently a significant amount of interest in identifying new materials for use as tunable solid state lasers. Thus far most of the research and development in this area has involved either 3d transition metal ions such as Cr, Co, and Ni in oxide hosts or color centers in alkali halide and oxide crystals. Another class of ions which may be useful in this application is the 4d and 5d transition metals and research is underway to survey the spectroscopic properties of these ions in different types of host crystals. This paper describes the results obtained on crystals of KCl:Ru^{2+}, KBr:Rh^{2+}, KCl:Ir^{2+}, and KBr:Pt^{2+}. Fluorescence intensities and lifetimes were measured as a function of temperature, annealing, and radiation treatment. The results are interpreted in terms of emission from both charge transfer states and excited d levels.

Extensive literature exists on the spectroscopic proper ties of 3d and 4d transition metal ions in chemical complexes.[1-4] Systematic studies have been performed on the spectral changes that occur with changes in the ligands and the structure of the chemical complex. Emission has been observed from charge transfer states, spin-allowed transitions from excited d levels, and spin-forbidden transitions from excited d levels. The two series of ions exhibit a variety of broad emission bands throughout the visible region of the spectrum. However very little work has been done on these ions as dopants in single crystals.[5-7] The goal of this work is to begin to understand the properties of 4d and 5d transition metal ions in crystals and to develop techniques for enhancing d level emission compared to

charge transfer emission.

(a) Samples

The crystals used in this project were grown by the Czochralski method of pulling from the melt. All growth was carried out in a dry nitrogen atmosphere in an internally heated furnace. Fisher Scientific reagent grade KBr and KCl were used for the host starting materials. The $PtCl_2$ (99.9%), $RhCl_3$ (99.9%), $IrCl_3$ (99.95%), and $RuCl_3$ (99.9%) anhydrous dopants were obtained from the Gallard-Schlesinger Co. The melts were contained in high purity alumina crucibles. After the crystals were grown, they were slowly cooled to room temperature over a 16 hour period. Samples were cleaved from the boule perpendicular to the growth axis so as to ensure uniform doping.

Example crystals were analyzed with an EDXA attachment on an electron microscope to determine the concentration and distribution of the doping ions and to detect the presence of other impurities. In addition, electron paramagnetic resonance measurements were made on example samples to determine the valence of the optically active ions. The results of these measurements indicate that the dopant ions are distributed uniformly at concentrations of around 200 ppm. No significant amount of other optically active impurities or other valence states of the dopant ions were detected.

The ions of interest in this study are $Rh^{2+}(4d^7)$, $Ru^{3+}(4d^4)$, $Pt^{3+}(5d^6)$, and $Ir^{3+}(5d^7)$. Partial crystal field energy level diagrams for these d^n electron configurations[9] are shown in Fig. 1. The figure is restricted to the lowest sets of energy levels

in the strong crystal field region since this area contains the transitions of interest in interpreting the observed spectra. For each case there is a low lying set of excited states which can give rise to spin-forbidden transitions to the ground state and a higher set of states which can produce spin-allowed transitions to the ground state. Interactions between the transition metal ion and its ligands result in charge transfer states which lie at higher energies with respect to the d levels shown in the figure.

(b) Experimental Apparatus

Measurements of the fluorescence spectra and lifetimes were made using a pulsed nitrogen laser for excitation. This provided a pump pulse at 337.1 nm which was about 10 ns in duration and 1 Å in halfwidth. The samples were mounted in a cryogenic refrigerator capable of controlling the temperature between about 10 K and room temperature. The fluorescence was focused onto the entrance slit of a 1-m monochromator with the slits set for 20 Å resolution. The signal was detected by a cooled RCA C31034 photomultiplier tube and analyzed by a boxcar integrator before being displayed on a strip chart recorder.

To measure lifetimes the window of the boxcar was set in the scanning mode with a time resolution of about 50 ns. The fluorescence spectra were recorded at fixed times after the excitation pulse. Both fast and slow emission bands were observed in these materials and this time-resolved fluorescence technique can be used to emphasize either one of these two types of emissions. Examples of the observed spectra are presented in

the following section. Because of the large difference in lifetimes, it is difficult to show both types of emissions on the same spectra. To overcome this problem, the spectra shown in the figures were obtained at 50 μs after the laser pulses using a 1 MΩ load resistance which distorts the timing of the spectra and allows both types of bands to be easily seen. Thus the absolute magnitudes of the spectral bands in these figures is not meaningful but the relative changes in intensities between samples or with different experimental conditions is accurate.

In the absorption spectra of these samples, it was not possible to detect any bands due to the doping ions. Only the normal absorption edges of the host crystals near 250 nm were observed. Excitation spectra taken with a xenon lamp and 1/4-m monochromator showed the major absorption in all of the samples to occur as a triple peaked band between about 280 and 400 nm. The Ir doped sample exhibited additional excitation bands in the 500 to 600 nm region of the spectrum.

A 2 MeV van de Graaff accelerator was used for radiation treatment of the samples.

II. EXPERIMENTAL RESULTS

(a) KBr:Pt

Figure 2 shows the fluorescence spectra obtained for Pt^{3+} in KBr crystals at room temperature and 10.2 K for a freshly cleaved surface and at room temperature for an aged surface. There are two distinct spectral regions: the relatively narrow band at 380 nm and the broad, structured band between about 425 and 850 nm. The former has a fluorescence lifetime of less than 20 ns

independent of temperature and is attributed to emission from the charge transfer state, whereas the latter band has a temperature dependent lifetime in the microsecond time regime and is attributed to transitions between triplet d levels. The structure in the broad band shows the presence of several different d to d transitions split into two major bands. The relative intensities of the fluorescence bands show that the fraction of the total emission occurring in the d to d transitions decreases with respect to that originating from the charge transfer state as the sample surface ages. At the same time the lower energy d emission band increases relative to the higher energy d emission band. These relative intensities also vary with temperature with the d to d emission relative to the charge transfer emission decreasing as temperature is lowered.

Figure 3 shows the temperature dependences of the emission intensities and lifetime for this sample. The ratio of the total emission from the d levels to that of the charge transfer level increases with temperature reaching a maximum at 250 K. Although both major d emission bands increase in intensity with temperature up to 250 K, the higher energy band increases more rapidly. Above this temperature the higher energy band decreases while the low energy band continues to increase with temperature. The solid lines in the figure represent the best fits to the data using the model discussed below.

(b) KBr:Rh^{3+}

Figure 4 shows the emission spectra of KBr:Rh^{3+} at room temperature for an as-grown sample, a crystal that has been exposed to a radiation dose of 10^8 rads of electrons, and a

sample that was annealed by heating to 600 C and fast cooling on a copper block. Again both charge transfer and spin allowed doublet d emission bands are observed. Both radiation and heat treatment enhance the d emission with respect to the charge transfer emission. The former treatment tends to preferentially increase the lower energy d band while the latter preferentially increases the higher energy d band.

Figure 5 shows the temperature dependences of the relative intensities and fluorescence lifetime of the d emission. The trends are similar to those discussed above for Pt except that the intensity ratios show a more pronounced maximum near 250 K. The solid line represents the theoretical fit discussed below while the dashed line simply shows the general trend of the intensity ratios. Again the lifetime of the charge transfer emission is less than 20 ns and no change with temperature could be observed within the time resolution of our instrumentation.

(c) $KCl:Ir^{3+}$

Figures 6 and 7 show the spectra and temperature dependences of the lifetimes and relative intensities for $KCl:Ir^{3+}$ crystals. The results are similar to those observed in the other samples except that the d emission intensity is much weaker in comparison to the charge transfer bands.

(d) $KCl:Ru^{3+}$

Figures 8 and 9 show the results obtained for $KCl:Ru^{3+}$ crystals. This case shows the weakest d emission compared to the charge transfer emission at room temperature. Unlike the other samples, this material shows a slight increase in the intensity

ratios as temperature is lowered.

III. INTERPRETATION

The spectroscopic results described in the last section are quite complex and obviously involve dynamic interactions among several different types of charge transfer and d levels. The exact details of these interactions can not be determined without more extensive experimental results but the general spectroscopic features can be interpreted in terms of the simplified single configuration coordinate model shown in Fig. 10. The manifold of crystal field split charge transfer states are represented by one potential curve and the system of d levels is represented by one ground state and two excited state potential curves. At low temperatures the absorption transition is followed by radiationless relaxation to the bottom of the charge transfer potential well. The majority of the emission occurs from this relaxed state. As temperature is raised, higher energy vibrational levels of the charge transfer state are occupied and when an energy ΔE_1 is reached, cross over occurs to the higher energy d level. Transfer to the lower d level occurs at a temperature consistent with ΔE_2 and fluorescence emission occurs from the bottom of both the d potential wells. At temperatures above that consistent with an energy ΔE_3 radiationless decay to the ground state occurs. The temperature dependences of the relative intensities and lifetimes depend on the energies ΔE_1, ΔE_2, and ΔE_3.

The intensity of the fluorescence emission from each level is proportional to the concentration of ions in the level, n_i. Representing all of the charge transfer states by one level

and all of the excited d states by one level, the rate equations of the excited state populations are

$$dn_{ct}/dt=W_{ct}-\tau_{ct}^{-1}n_{ct}-\beta n_{ct}$$
$$dn_d/dt=W_d-\tau_d^{-1}n_d+\beta n_{ct} \quad (1)$$

where the W_i represent the pumping rates, the τ_i are the fluorescence lifetimes, and β is the radiationless relaxation rate between the two sets of levels. These equations can be solved simultaneously and the resulting expressions for the time dependences of the excited state populations are directly proportional to the measured fluorescence intensities. This procedure provides equations for fitting the experimental data on the temperature variations of the fluorescence lifetimes and relative intensities.

The temperature dependences of the ratios of fluorescence intensities at a specific time after the excitation pulse can be expressed as

$$I_d/I_{ct}=A+B\exp(-\Delta E_i/kT). \quad (2)$$

The temperature independent coefficients A and B contain factors describing the ratios of the initial pumping rates and the radiative decay rates of the two types of levels as well as a correction factor for the detection sensitivity in the different spectral ranges of the two types of emissions and an exponential time factor. The exponential temperature dependence comes from expressing the parameter β as the ratio of the rates of absorption and emission of phonons coupling the charge transfer and d states.

The solid line in Fig. 3 represents the best fit to the

temperature dependent intensity data for KBr:Pt using Eq. (2) and treating A, B, and ΔE_1 as adjustable parameters. This fit was obtained for A=1.69, B=240, and ΔE_1=398 cm^{-1}. The simple model used here can not explain the peak in the intensity ratios at 250 K which is associated with the redistribution of energy among the several different ct and d levels which are present in the sample.

Similar good fits to the observed temperature dependences of the intensity ratios could not be obtained for the other samples. In the case of KBr:Rh the peak at 250 K is too dominant to allow the simplified model to be a good approximation. For KCl:Ir the strong increase with temperature begins to occur near 300 K. This indicates a higher value of E_1 but the measurements do not extend to high enough temperatures to obtain an accurate theoretical fit. The temperature dependence of the intensity ratios for KCl:Ru is the opposite of that predicted by the simple model used here which is probably due to redistribution of the energy among different types of charge transfer states with different radiative emission rates. Some evidence for this can be seen in the spectra shown in Fig. 8.

The temperature dependences of the fluorescence lifetimes of the d emission bands can be interpreted by a model assuming the presence of two d levels with different intrinsic decay times τ_{LT} and τ_{HT} separated by an energy barrier, ΔE_2, and connected by efficient radiationless processes so that the populations of the levels are in thermal equilibrium. For this situation the observed fluorescence decay time will be the weighted combination of the two intrinsic decay times

$$\tau = \{1+G\exp(-\Delta E_a/kT)\}/\{(1/\tau_{LT})+(1/\tau_{MT})G\exp(\Delta E_a/kT)\} \quad (3)$$

where G is the ratio of the degeneracies of the two states. This equation gives a reasonably good fit to the lifetime data for all four samples as shown in Figs. 3, 5, 7, and 9. The solid lines are obtained treating G, ΔE_a, and the two intrinsic lifetimes as adjustable parameters. The numerical results for these parameters are listed in Table 1. The values obtained are physically reasonable except for the value of G=50 for KBr:Pt. This high value indicates that the structure of the d manifold of levels is more complex than the simple model employed here.

The changes in sample properties after various types of treatments are associated with the defect structure of the material. When divalent ions are incorporated in alkali halide crystals, charge compensation is necessary. Usually this takes the form of alkali ion vacancies which are not necessarily located close to the dopant ions. These defects are mobile and aging, annealing, and radiation treatments can cause the formation and redistribution of defect centers. The spectral changes observed for the samples studied here due to these types of treatments can be attributed to the effects of the interaction of the dopant ion with near neighbor lattice defects. The position and shape of the charge transfer potential well is especially sensitive to changes in the ligand structure in the environment of the transition metal ion. Shifting this potential well can significantly change the efficiency of radiationless transfer from the charge transfer state to the d levels. The spectra shown in Figs. 3 and 5 indicate that local charge

compensation greatly enhances the cross over to the d levels. Similar results were observed on other samples such as KCl:Ru. However, no significant changes in the spectrum were observed in a sample of $KMgF_3$:Rh after annealing. This is due to the fact that the defect mobility in $KMgF_3$ crystals is greatly reduced compared to alkali halides.

IV. DISCUSSION AND CONCLUSIONS

Table 1 summarizes the spectral properties of the four samples studied in this work. The results indicate that the energy levels and dynamics of 4d and 5d transition metal ions in alkali halide crystals are quite complex. The spectra shown in Figs. 2, 4, 6, and 8 show structure indicating the existence of several different types of excited state levels and the significant changes observed with variations in temperature or different types of sample treatment indicate that the population dynamics of these levels is extremely sensitive to the local environment of the dopant ion and to lattice vibrations. The simplified configuration coordinate model proposed here is useful in interpreting some of the general spectral properties but additional, systematic studies are necessary to gain a complete understanding of these materials.

The identification of the peaks appearing in the near uv spectral region as being due to charge transfer transitions and the peaks in the visible spectral region as being due to spin-allowed d-d transitions is somewhat arbitrary. However these assignments are consistent with the observed strengths of these peaks in absorption and with their fluorescence lifetimes as compared to the values of these parameters generally measured for

these different types of transitions. In addition, the overall spectral properties of these materials are similar to those observed for these ions in chemical complexes[1-4] where much work has been done to unambiguously identify the bands belonging to charge transfer and d-d transitions. A similar definitive assignment for the materials investigated here must await further experiments to provide conclusive information about the local structure and ligand interactions in these crystalline environments. Since the materials investigated here contain lattice vacancies necessary for charge compensation of the doping ions, and since radiation treatment is used to alter the spectral characteristics of the samples, it is important to note that the spectral properties of color centers in these alkali halide host crystals are well known[9], and none of the reported spectral features are consistent with color center transitions.

The general location of the charge transfer bands is approximately the same for both of the 4d and both of the 5d transition metal ions in the two types of alkali halide host crystals. However, the exact peak positions, widths and structure of these bands are different for each sample. For example, the ct bands in both KCl samples appear as two extremely narrow transitions whereas in both KBr samples they are broader, single transitions. This demonstrates the general similarity of the host-impurity ion systems and the effects of different ligands on the spectral details. These results are again similar to those obtained on chemical complexes of these ions.[1-4]

For a detailed spectral analysis of these 4d and 5d

transition metal ions in solids, it would be desirable to obtain specific information on the local crystal field at the site of the ions. In this case it is difficult to do for two reasons: the very weak d-d absorption transitions and the lack of information on the free ion Racah parameters for these particular ions. Of the four ions investigated, the free ion B parameter is known only for Rh^{3+} and its value is[10] 620 cm^{-1}. If the structure in the broad emission band in Fig. 4 is interpreted as due to transitions from the crystal field split components of the $^2T_2$ and $^2T_1$ levels, the average value of the two lowest energy peak positions can be used as an estimate of the position of the $^2T_1$ energy level in an octahedral field. Dividing this energy by the published value of B given above provides a value for E/B to use in the crystal field diagram for d^7 ions shown in Fig. 1. This leads to a cubic crystal field parameter of Dq=1,460 cm^{-1}. This must be considered only as an estimate of the lower bound of Dq since it was obtained from fluorescence peak positions and these transitions are known to undergo a large Stokes shift between absorption and emission. The only published value of Dq for Rh^{3+} is 1,600 cm^{-1} in $ZnWO_4$ crystals.[11] This is consistent with the lower bound, Stokes shifted value of Dq given above. More accurate crystal field analysis of these materials requires samples with higher concentrations of doping ions so that the positions of d-d absorption transitions can be accurately determined.

The broad d emission bands for these materials are attractive possibilities for tunable laser applications. One critical parameter for this consideration is the peak emission

cross section given by

$$\sigma_p = (0.02\lambda_p^2 \eta) / (n^2 \Delta\nu\tau_r) \quad (4)$$

where λ_p is the peak wavelength of the emission band and $\Delta\nu$ is its frequency half width. η is the quantum efficiency. The latter quantity is difficult to determine accurately since no temperature dependent intensity quenching is observed in the temperature region studied. In calculating σ_p a value of 0.5 was used for which should be a good approximation in comparison to previous results on chemical complexes of these ions. The values obtained for the cross sections are listed in Table 1 and are all of the order of $10^{-21}cm^{-1}$ which is similar to σ_p for 3d ion transition metal vibronic laser materials. The lifetimes of the order of tens of microseconds indicate that fast laser pumping would be better than flashlamp pumping of these materials. This type of pumping should be very efficient since these materials have strong charge transfer absorption bands coincident with the N_2 laser wavelength. To test these materials as lasers, crystal growth techniques are being developed to incorporate an order of magnitude higher concentration of dopant ions in the host crystals. No evidence for emission from the low energy states with spin forbidden transitions was observed in these host crystals. There is some evidence that intersystem crossing to these levels is more efficient in oxide crystal hosts[8] and samples of this type are under preparation. These transitions should have millisecond lifetimes and be better suited for flashlamp pumped laser applications.

In conclusion, this work demonstrates the existence of both

charge transfer and d level fluorescence emission from 4d and 5d transition metal ions in alkali halide crystals. It also shows how the d emission can be enhanced through thermal or radiation treatments resulting in broad fluorescence bands throughout the visible region of the spectrum. These materials may be useful in tunable laser applications if samples can be prepared with high enough levels of doping.

ACKNOWLEDGMENTS. This research was supported by the Office of Naval Research and the U.S. Army Research Office. The authors express their appreciation to L.E. Halliburton, Z.F. Al Shaieb, and G.D. Gilliland for technical assistance in this work and to W.A. Sibley for helpful discussions concerning the interpretation of the results.

TABLE 1. Spectroscopic Parameters

PARAMETER	CRYSTAL			
	KCl:Ru ($4d^4$)	KBr:Rh ($4d^7$)	KCl:Ir ($5d^7$)	KBr:Pt ($5d^8$)
λ_p(nm)	588	650	636	660
$\Delta\lambda$(nm)	268	270	226	216
τ_f(μs)	46	25	35	23
σ_p($10^{-21}cm^2$)	1.16	2.10	2.50	3.27
ΔE_2(cm^{-1})	275	355	350	700
τ_{LT}(μs)	99	80	78	110
τ_{HT}(μs)	19	13	12.4	13.7
G	5	3.75	2.5	50

REFERENCES

1. G.A. Crosby, W.G. Perkins and D.M. Klassen, J. Chem. Phys. 43, 1498 (1965); K.W. Hipps, G.A. Merrell, and G.A. Crosby, J. Phys. Chem. 80, 2232 (1976); J.N. Demas and G.A. Crosby, J. Am. Chem. Soc. 92, 7262 (1970); ibid, 93, 2841 (1971); W.A. Fordyce and G.A. Crosby, ibid, 21, 1455 (1982).
2. R.J. Watts and G.A. Crosby, J. Am. Chem. Soc. 94, 2606 1972); T.R. Thomas, R.J. Watts, and G.A. Crosby, J. Chem. Phys. 59, 2123 (1973); R.J. Watts and D. Missimer, J. Am. Chem. Soc. 100, 5350 (1978).
3. W. Halper and M. K. DeArmond, J. Lumin. 5, 225 (1972).
4. F. Diomedi Camassei, L. Ancarani-Rossiello, and F. Castelli, J. Lumin. 8, 71 (1973).
5. G. Blasse and A. Bril, J. Electrochem. Soc. 114, 1306 (1967).
6. C.D. Plint and A.G. Poulusz, Molecular Phys. 41, 907 (1980).
7. W. Holzapfel, H. Yersin, and G. Gliemann, J. Chem. Phys. 74, 2124 (1981).
8. S. Sugano, Y. Tanabe, and H. Kamimura, Multiplets of Transition-Metal Ions in Crystals, (Academic Press, N.Y., 1970).
9. A.E. Hughes, D. Pooley, H.U. Rahman, and W.A. Runciman, "A Survey of Radiation DFamage and Related Phenomena in the Alkali Halides", United Kingdom Atomic Energy Research Establishment Report R5604, 1967.

10. B. DiBartolo, "Optical Interactions in Solids", (John Wiley, New York, 1968).

11. M.G. Townsend, J. Chem. Phys. 41, 3149 (1964).

FIGURE CAPTIONS

Fig. 1. Portions of crystal field crystal field energy level diagrams for d^4, d^7, and d^8 ions in octahedral environments.

Fig. 2. Fluorescence spectra of KBr:Pt after pulsed N_2 laser excitation. —— 300 K, freshly cleaved sample; – – – 10 K freshly cleaved sample; •••• 300 K aged sample.

Fig. 3. Temperature dependences of the fluorescence lifetime of the d emission and the ratios of the integrated intensities of the d and charge transfer emissions for KBr:Pt. See text for explanation of the theoretical lines.

Fig. 4. Fluorescence spectra of KBr:Rh at 300 K after pulsed N_2 laser excitation. – – – untreated sample; —— irradiated sample; ••••• annealed sample.

Fig. 5. Temperature dependences of the fluorescence lifetime of the d emission and the ratios of the integrated intensities of the d and charge transfer emissions for KBr:Rh. See text for explanation of the theoretical curve.

Fig. 6. Fluorescence spectra of KCl:Ir after pulsed N_2 laser excitation at 10 K (– – –) and room temperature (——).

Fig. 7. Temperature dependences of the fluorescence lifetime of the d emission and the ratios of the integrated intensities of the d and charge transfer emissions for KCl:Ir. See text for explanation of the theoretical curve.

Fig. 8. Fluorescence spectra of KCl:Ru after pulsed N_2 laser excitation at 10 K (——) and room temperature (– – –).

Fig. 9. Temperature dependences of the fluorescence lifetime of the d emission and the ratios of the integrated intensities of the d and charge transfer emissions for KCl:Ru. See text for explanation the the theoretical curve.

Fig. 10. Simplified single configuration coordinate model for interpreting the experimental results.

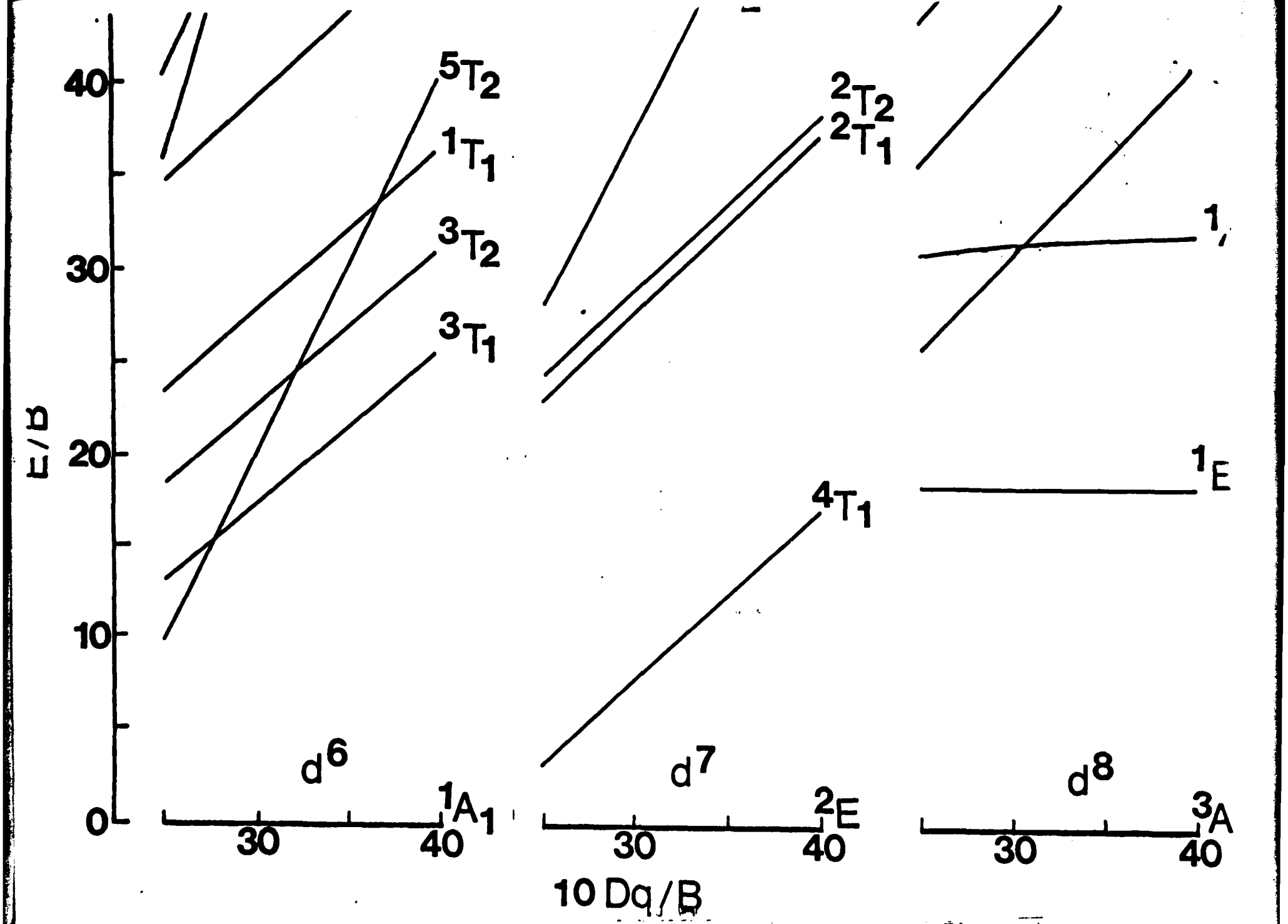
E/B
40
30
20
10
0
$^5T_2$
$^1T_1$
$^3T_2$
$^3T_1$
$^2T_2$
$^2T_1$
$^4T_1$
^1E
d^6
$^1A_1$
d^7
^2E
d^8
^3A
30
40
10 Dq/B

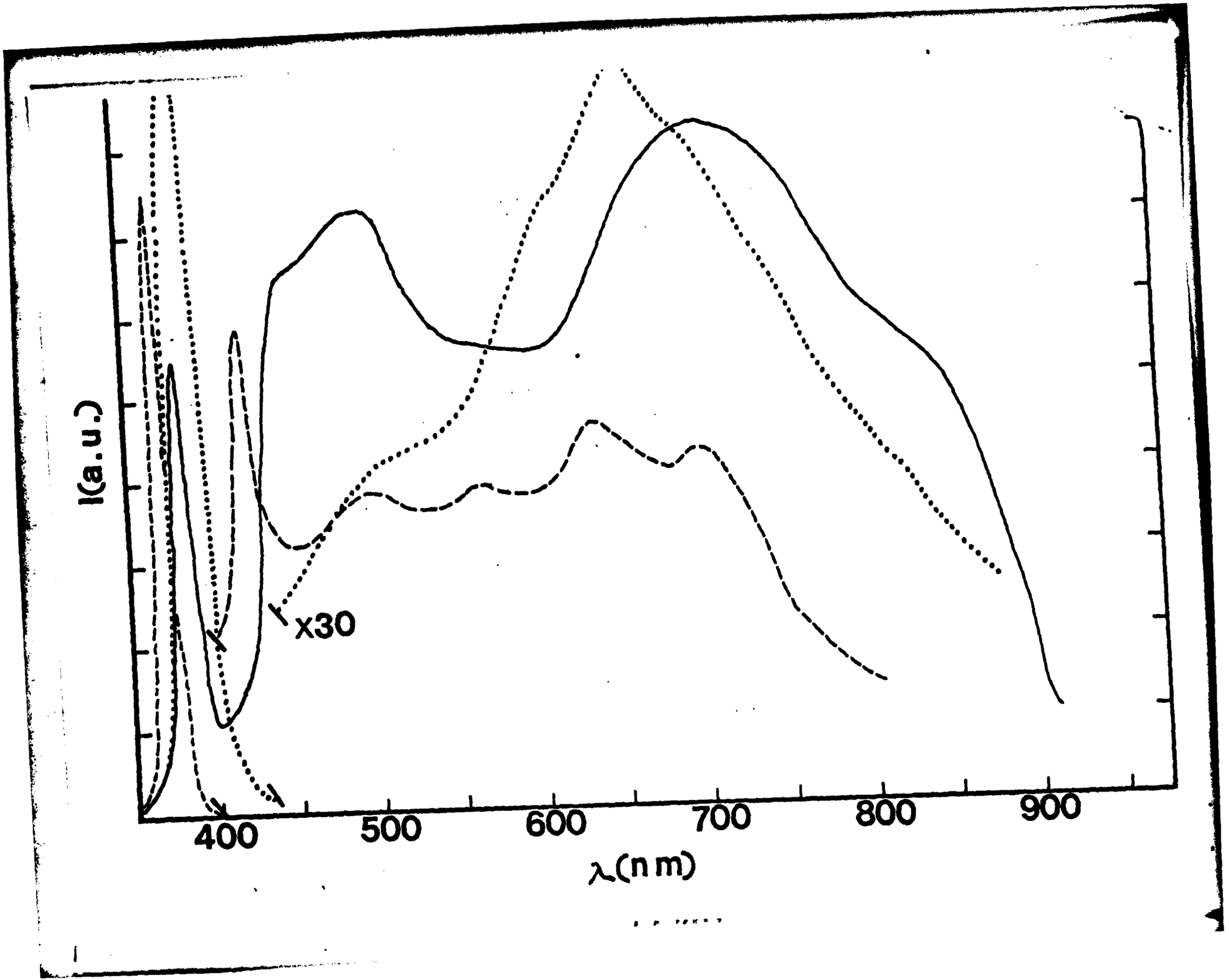
I(a.u.)
x30
400
500
600
700
800
900
λ(nm)

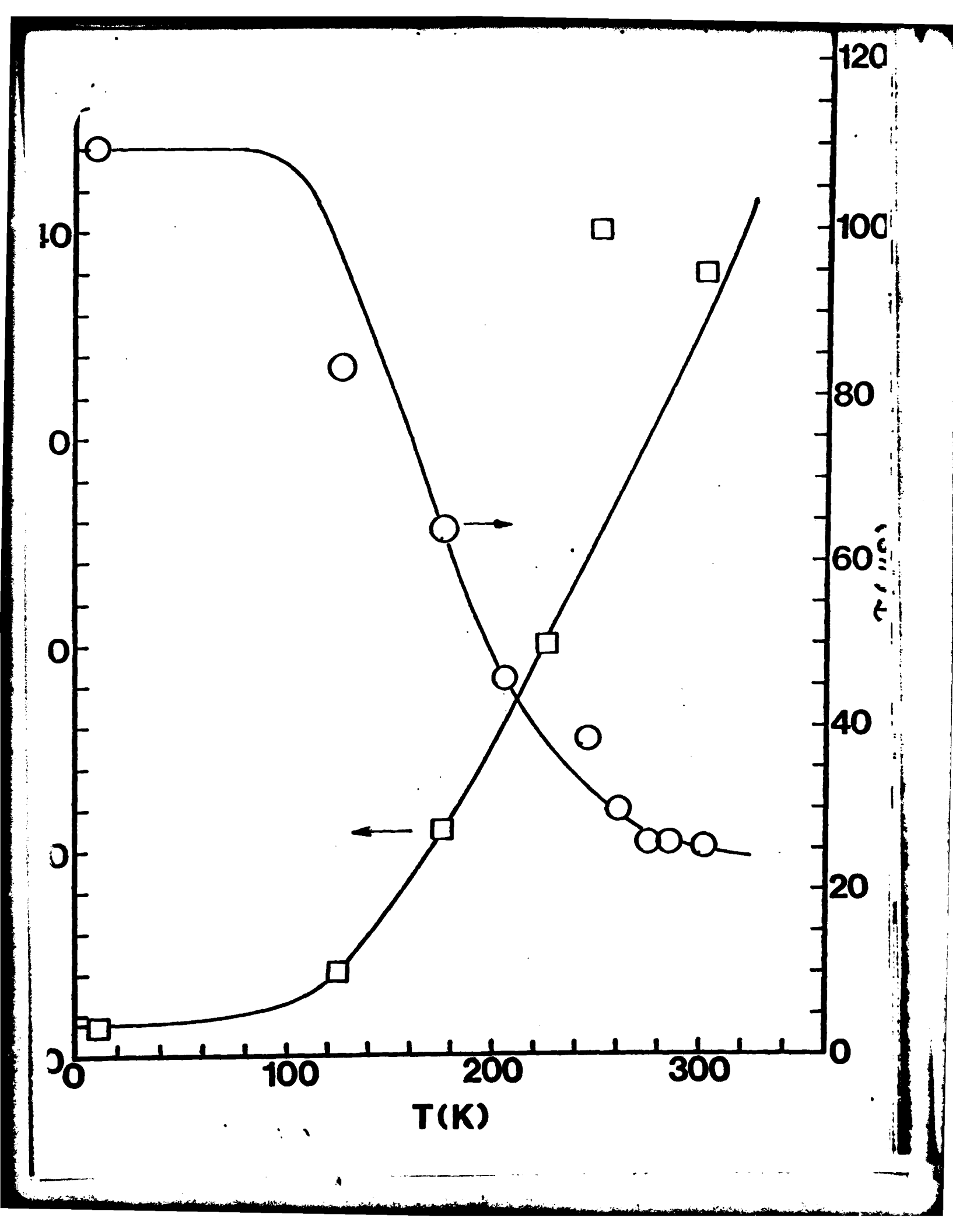
120
100
80
60
40
20
0
100
200
300
T(K)

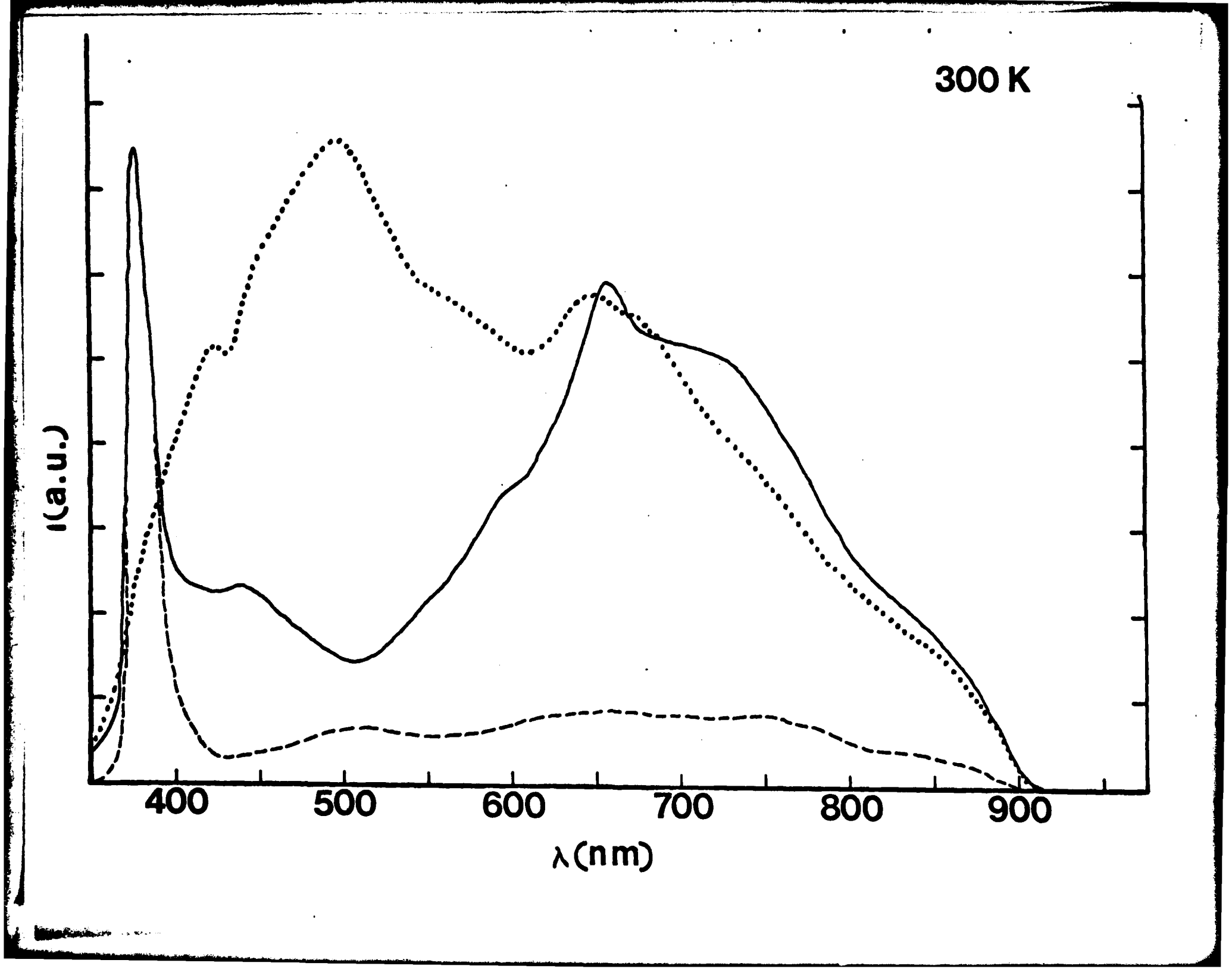
300 K
I(a.u.)
400
500
600
700
800
900
λ(nm)

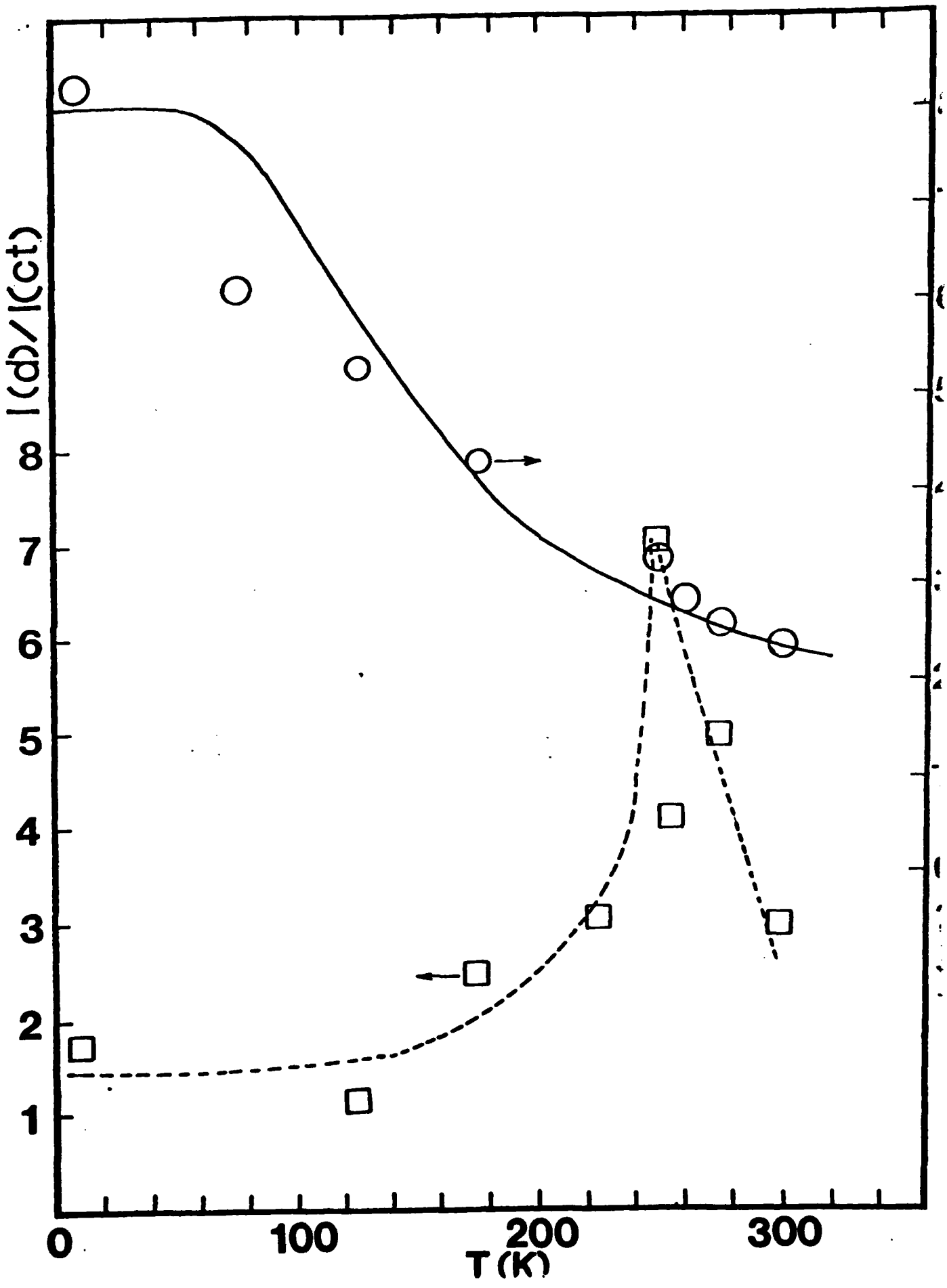
I(d)/I(ct)
8
7
6
5
4
3
2
1
0
100
200
300
T (K)

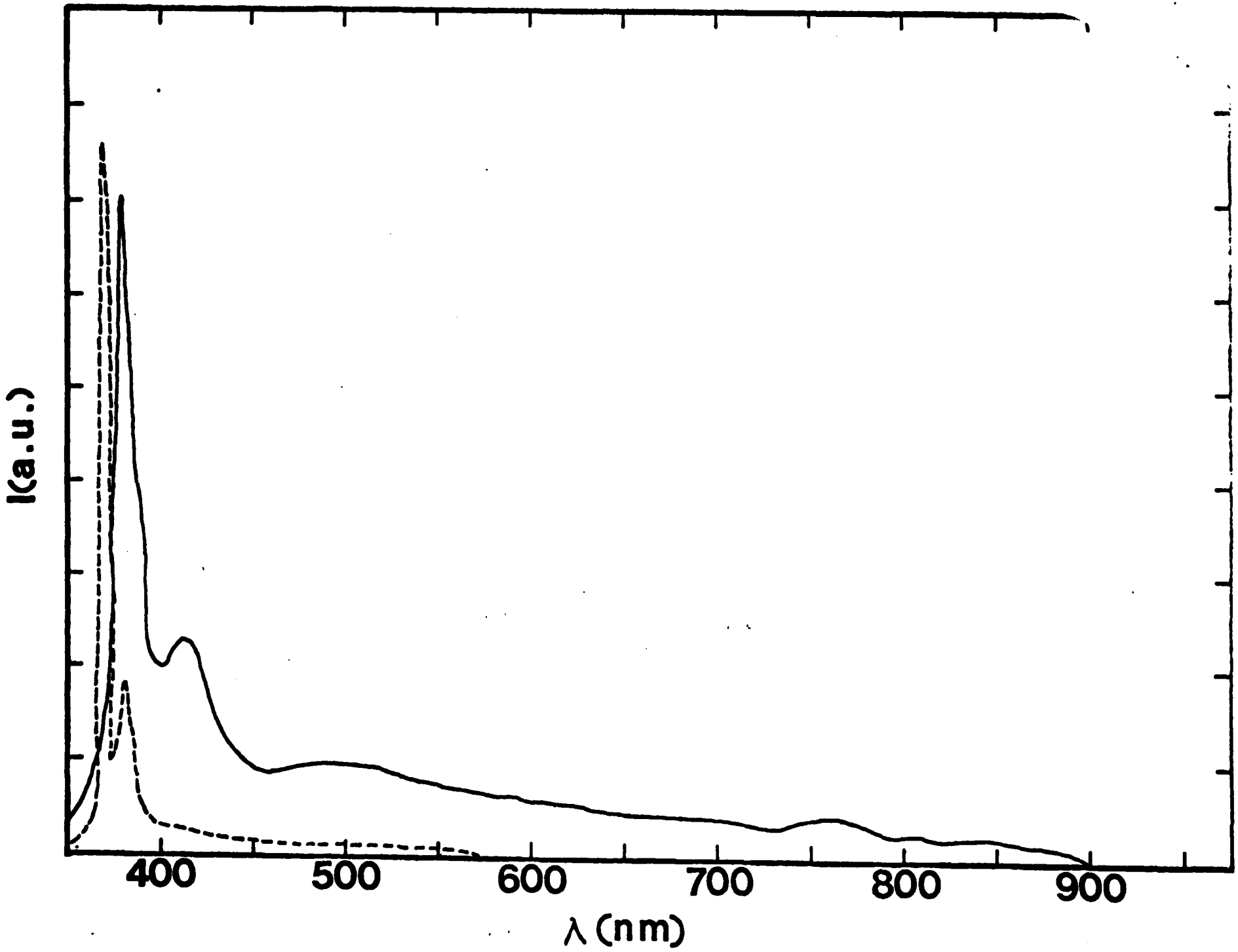
I(a.u.)
400
500
600
700
800
900
λ (nm)

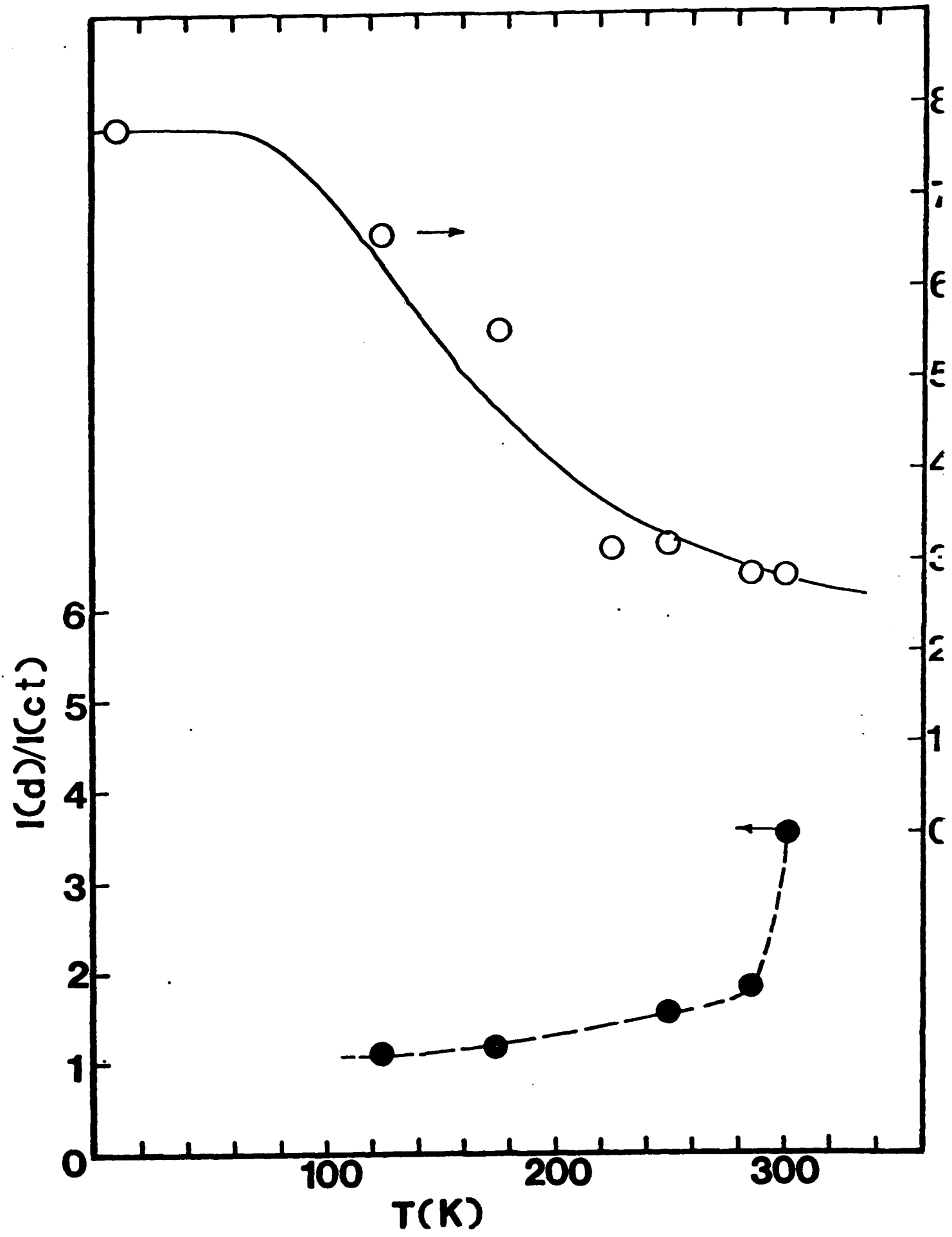
I(d)/I(ct)
0
1
2
3
4
5
6
100
200
300
T(K)

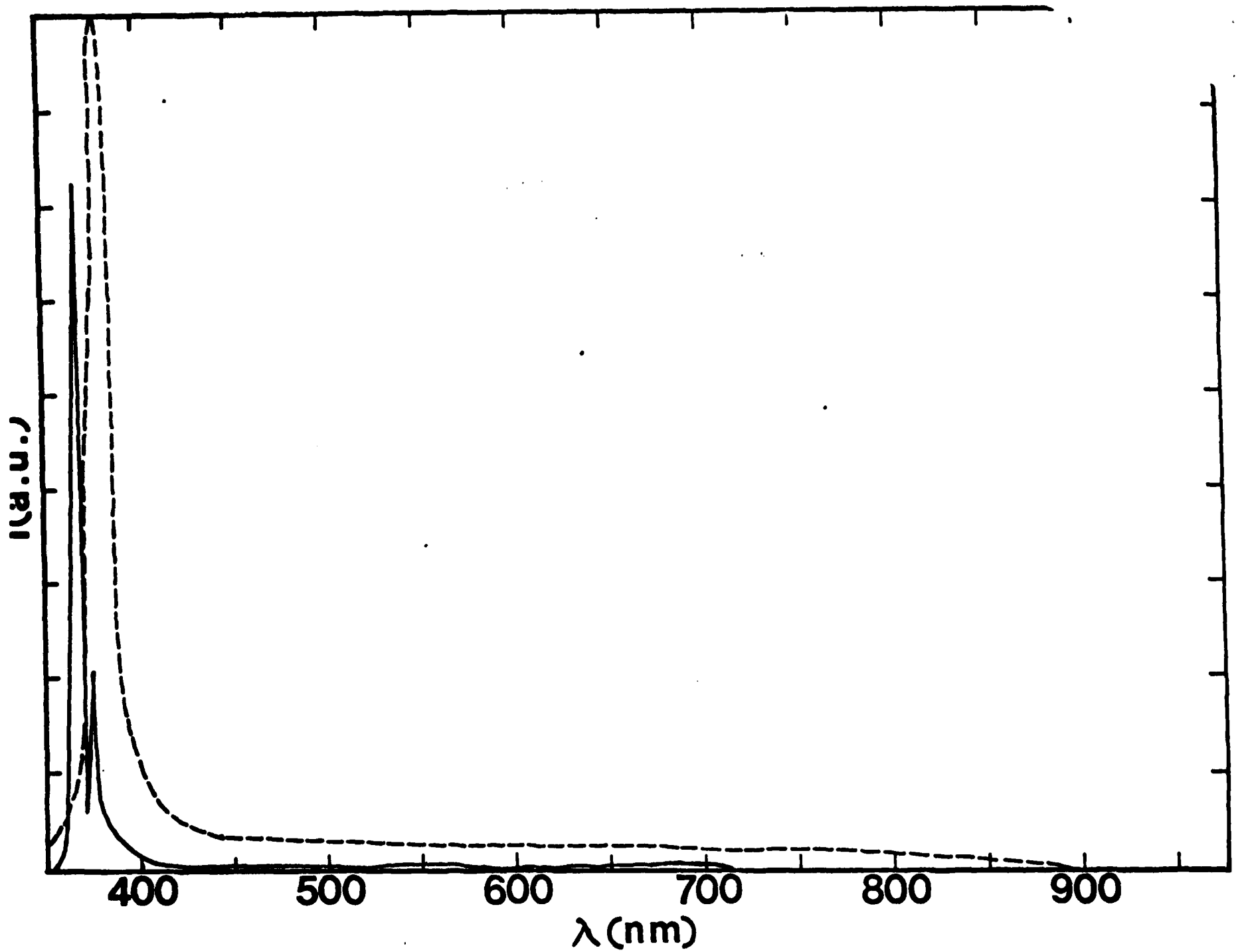
I(a.u.)
400
500
600
700
800
900
λ(nm)

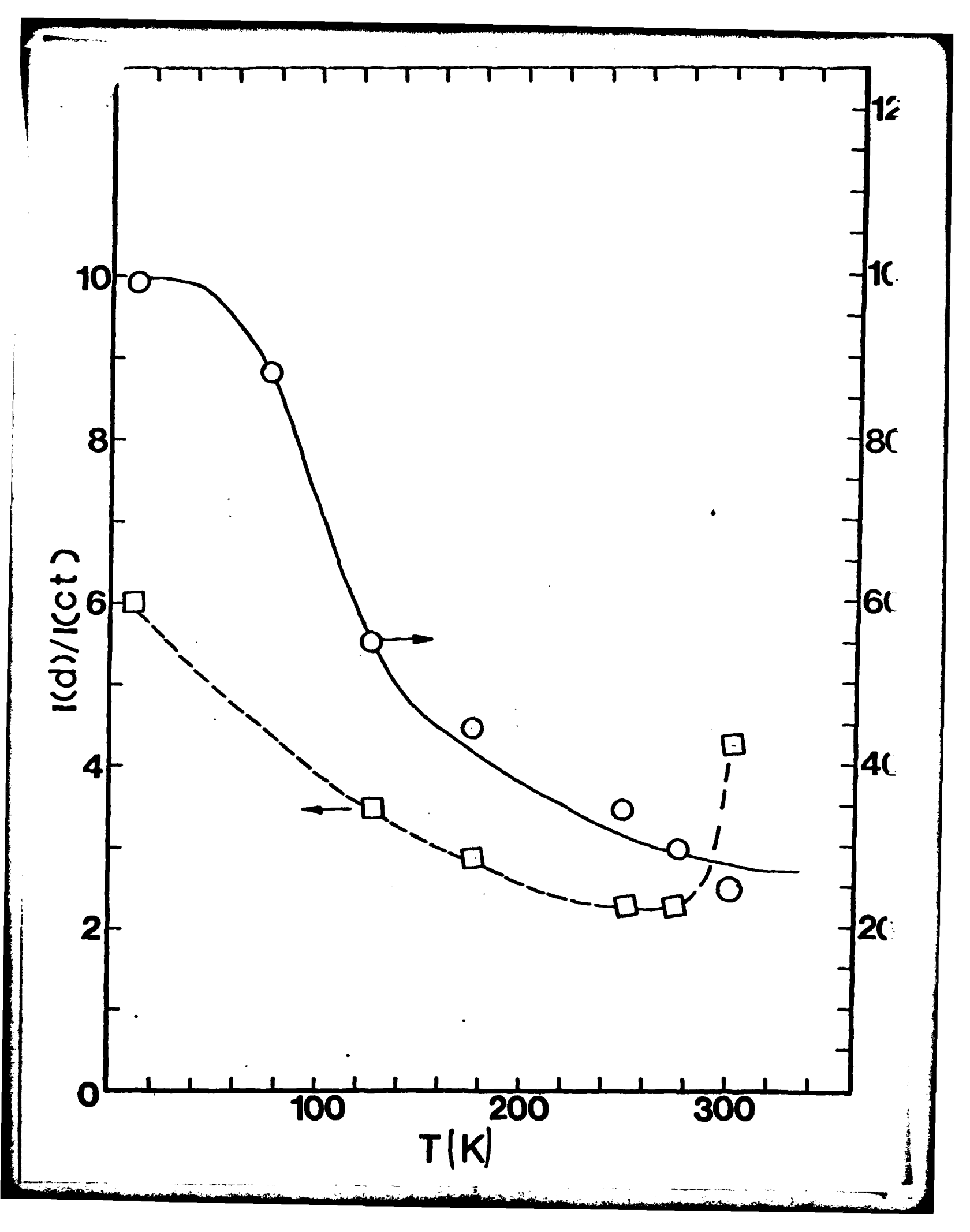
I(d)/I(ct)
T(K)
0
2
4
6
8
10
12
100
200
300

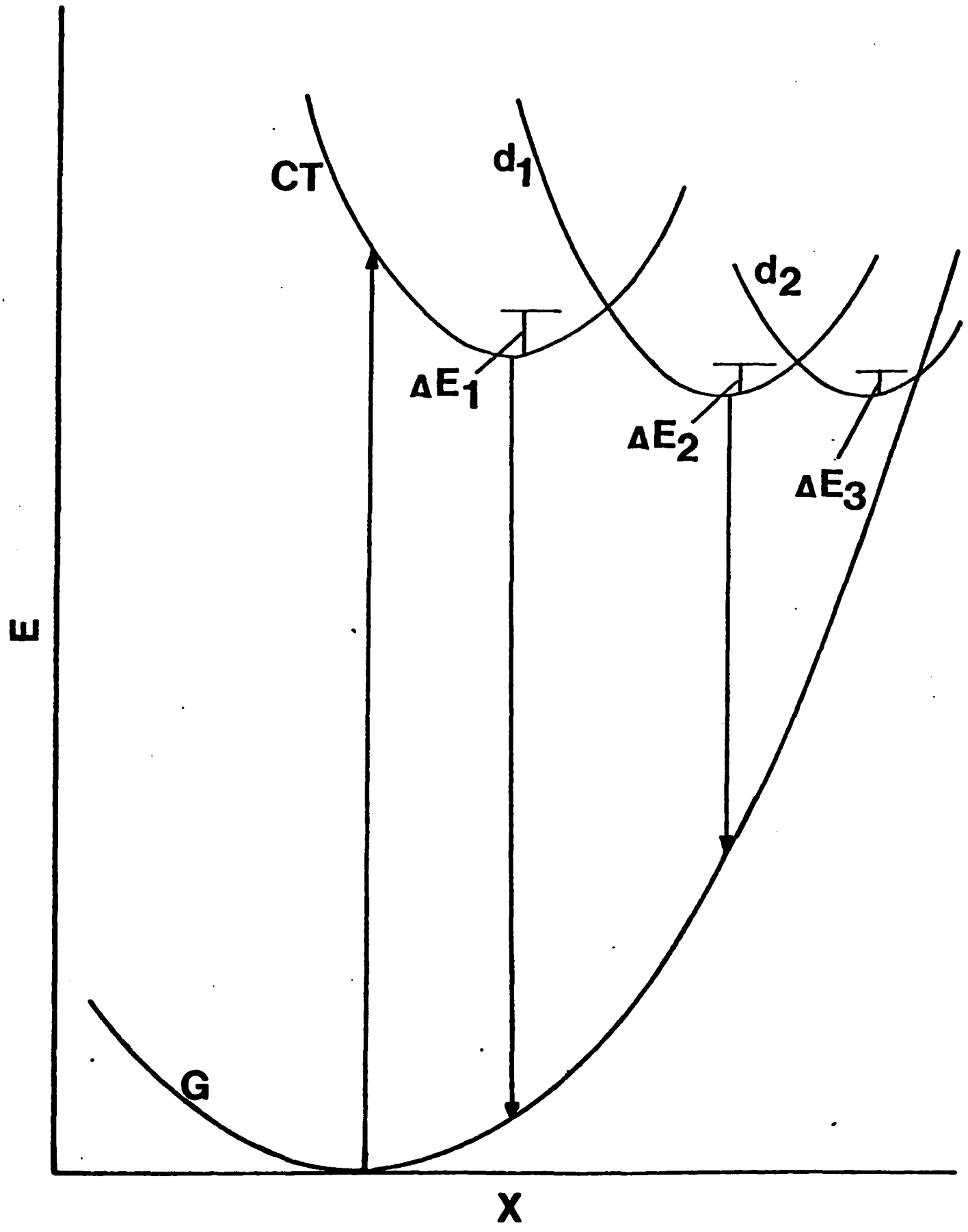
CT
d1
d2
ΔE1
ΔE2
ΔE3
E
G
X

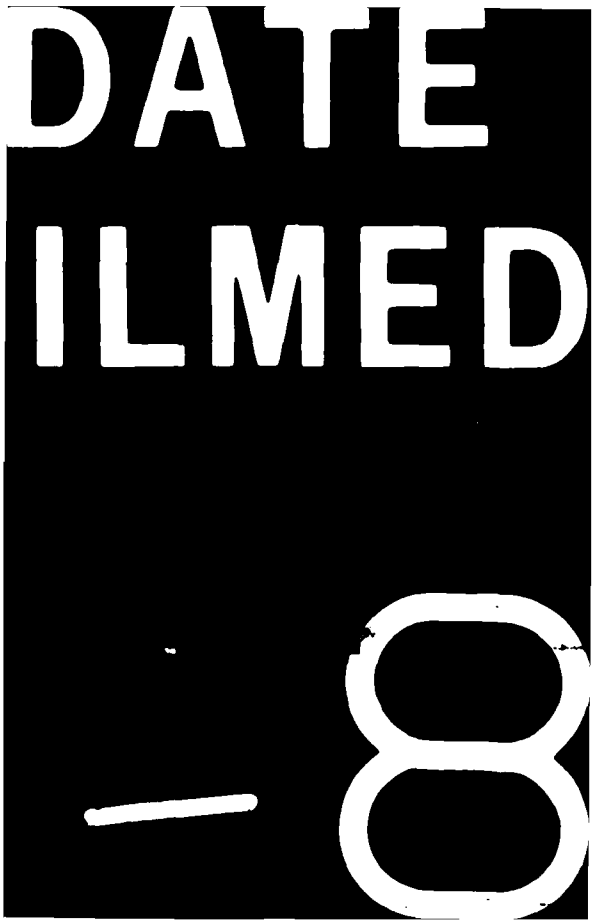
DATE
ILMED
-8